Zitierweise: *Angew. Chem. Int. Ed.* **2024**, *63*, e202405091
doi.org/10.1002/anie.202405091

Foldamers **Hot Paper**

Domain Swapping in Abiotic Foldamers

*Shuhe Wang, Barbara Wicher, Céline Douat, Victor Maurizot, and Ivan Huc**

Abstract: Foldamer sequences that adopt tertiary helix-turn-helix folds mediated by helix-helix hydrogen bonding in organic solvents have been previously reported. In an attempt to create genuine abiotic quaternary structures, i.e. assemblies of tertiary structures, new sequences were prepared that possess additional hydrogen bond donors at positions that may promote an association between the tertiary folds. However, a solid state structure and extensive solution state investigations by Nuclear Magnetic Resonance (NMR) and Circular Dichroism (CD) show that, instead of forming a quaternary structure, the tertiary folds assemble into stable domain-swapped dimer motifs. Domain swapping entails a complete reorganization of the arrays of hydrogen bonds and changes in relative helix orientation and handedness that can all be rationalized.

Driven by curiosity and creativity, chemists have demonstrated that some folding patterns found in peptides and proteins can be reproduced in completely abiotic oligomers, that is, synthetic molecules chemically remote from aliphatic peptides. Abiotic oligomers also have features of their own, such as folding in organic medium, that can be put to an advantage. For example, aromatic helices with a variable diameter may completely surround a guest,[1–4] while open-ended helices selectively channel molecules or ions through bilayer membranes.[5–9] Early examples of abiotic foldamers comprised isolated secondary structural elements, i.e. helices, linear strands or turns.[10–16] Several such elements were then connected,[17–19] eventually generating the first true abiotic tertiary structures under the form of helix-turn-helix folds.[20–22] These model systems reproduce effects well-known in proteins. For example, abiotic tertiary structures may cooperatively stabilize secondary folds, e.g. helices too flexible to fold well on their own.[23] Conversely, tertiary structures may frustrate secondary folding and accommodate a certain level of strain.[24] Both cooperativity and frustration may promote dynamic changes beneficial to function, as they do in proteins. Here, we present the rare observation in abiotic structures of yet another phenomenon common in proteins, namely domain swapping.[4]

Protein tertiary structures consisting of at least two domains, that is, two subparts whose folds are inherently stable, may undergo multimerization through domain swapping.[25,26] While the domains bind to each other intramolecularly in a protein monomer, they may bind intermolecularly through the same or similar interactions in the domain-swapped multimer. Entropy expectedly favors monomers. Domain swapping is therefore the reflection of additional driving forces that favor multimers. Our discovery of domain swapping in abiotic foldamers stemmed from an attempt to produce the first genuine abiotic quaternary structures, i.e. aggregates of tertiary folds.

In organic solvents, oligoamide sequences of aromatic δ-amino acids of general formula Q and P (Figure 1a) have been shown to fold into stable helices. The amide carbonyl oxygen atoms diverge from these helices and provide hydrogen bond acceptors at their surface (Figure S1).[27–29] Adding complementary hydrogen bond donors such as the 4-hydroxy groups of monomers X and Y (Figure 1a), at precise positions at the surface of the helices promotes tight hydrogen bond-mediated helix-helix associations in chlorinated solvents.[20,22,30] Furthermore, turn units such as monomer T2 (Figure 1a) can be placed between two helix segments within a sequence to induce the formation of a helix-turn-helix tertiary motif.[20–22] Thus, X-, Y- and T2-containing sequence **1** (Figure 1b) folds as depicted in Figure 2a, forming a helix-turn-helix structure stabilized by six inter-helix hydrogen bonds (Figures S2, S3). Three features of the structure of **1** should be highlighted here. First, the axes of the two helices form strictly parallel lines (with head-to-tail orientation). Second, the effect of T2 is such that forming the six hydrogen-bonds requires an inversion of helix handedness (Figure 2a).[21] If the N-terminal helical segment of **1** (before T2) is right-handed (*P*), the C-terminal helix (after T2) must be left-handed (*M*), and reciprocally. Third, and important in the context of this study, the helix-turn-helix structure of **1** is frustrated in that it forces the helices to deviate from their natural curvature to establish the hydrogen bonds.[24] Upon removing T2, different inter-helix hydrogen bonds take place. Specifically, because the six hydrogen-bond donors and the

[*] S. Wang, Dr. C. Douat, Prof. Dr. I. Huc
Department of Pharmacy,
Ludwig-Maximilians-Universität in Munich,
Butenandtstr. 5–13, 81377 München (Germany)
E-mail: ivan.huc@cup.lmu.de

Dr. B. Wicher
Department of Chemical Technology of Drugs,
Poznan University of Medical Sciences,
3 Rokietnicka St., 60-806 Poznan (Poland)

Dr. V. Maurizot
CBMN (UMR 5248), Univ. Bordeaux, CNRS, Bordeaux INP
2, Rue Robert Escarpit, 33600 Pessac (France)

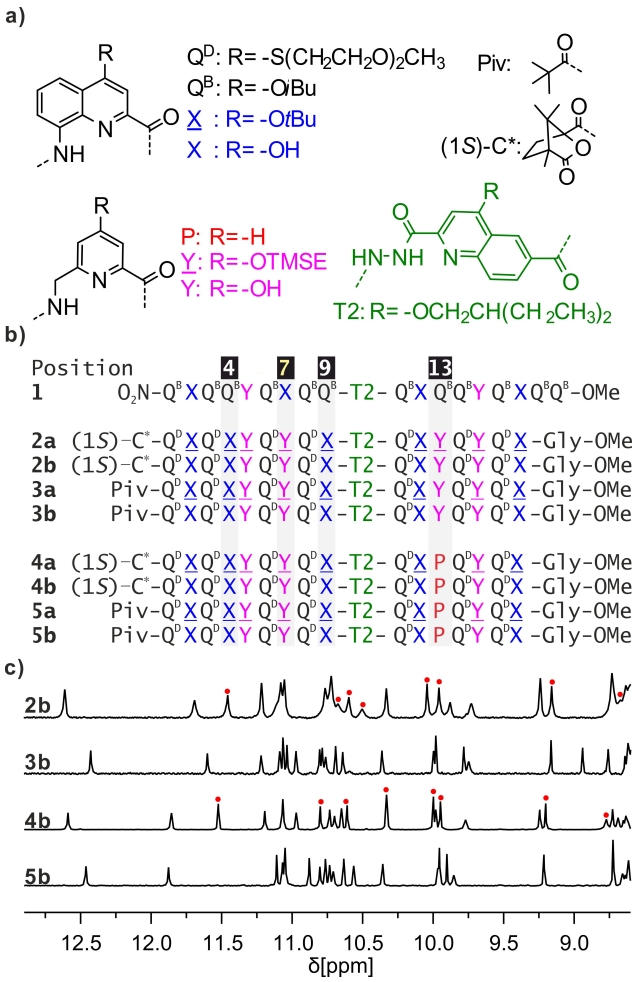

Figure 1. a) Structures of Q^B, Q^D, X, P, Y and T2 amino acid monomers as well as N-terminal Piv and (1*S*)-C* groups. X and Y are the protected precursors of X and Y, respectively. TMSE = 2-trimethylsilylethyl. The side chains of T2, Q^B and Q^D promote solubility in organic solvents. b) Oligoamide foldamer sequences. Gly stands for glycine. In **1**, the nitro group at the N-terminus replaces the NH group. c) Extracts of ^{1}H NMR spectra (500 MHz, 25 °C) of **2b**, **3b**, **4b** and **5b** in $CDCl_3$ showing the amide NH and hydrogen-bonded OH proton resonances. Signals assigned to OH protons are marked with red dots.

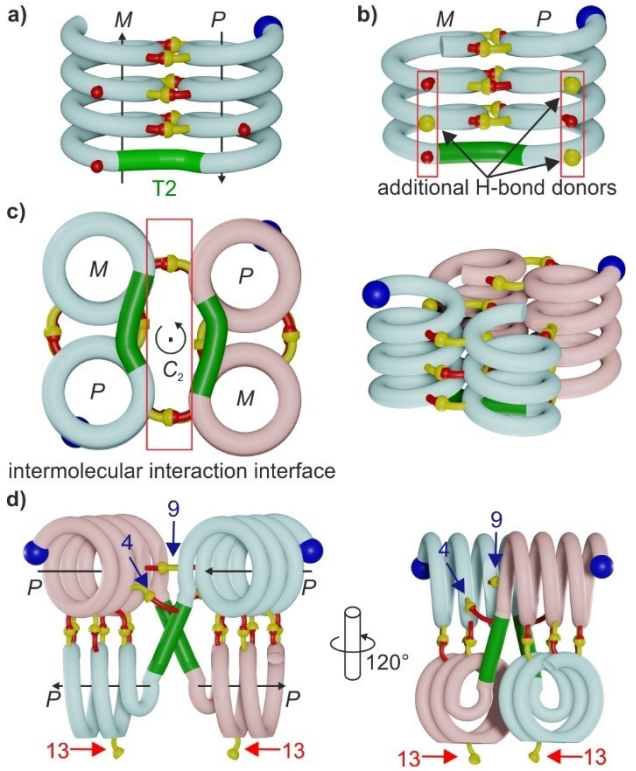

Figure 2. a) Schematic representation of a helix-turn-helix tertiary structure with a reversal of helix handedness. The N-terminus is marked with a blue ball. The T2 linker is shown in green. Red and yellow balls indicate hydrogen bond acceptors (carbonyl oxygen atoms) and donors (hydroxy protons), respectively. b) Modification of the structure in a) so as to create additional complementary arrays of hydrogen bonds (donor-acceptor-donor and acceptor-donor-acceptor shown in red boxes). c) Schematic representations of a hypothetical C_2-symmetrical dimer of the structure in b) preserving the helix-turn-helix fold. d) Representations of the observed domain-swapped dimer of the structure in b), this time without helix handedness reversal. Blue arrows point to unexpected hydrogen bonds. Red arrows point to hydroxy groups not involved in hydrogen bonds. In c) and d), two identical molecules are shown in pink and light blue.

six acceptors of the structure of **1** are arranged in a somewhat distorted hexagon, helices can also associate when their axes have been tilted by 120° in one or the other direction, forming so-called clockwise or counter-clockwise tilted dimers (Figure S4) that are more stable than parallel arrangements.[20,24] In summary, the helix-turn-helix structure of **1** promoted by the T2 turn forms despite the existence of better hydrogen bonding arrangements.

New sequences **2b** and **3b** (Figure 1b) are analogues of **1** with additional hydroxy groups at residues 4, 9, and 13 (Figure 1b). These hydroxy groups were placed on one face of the helix-turn-helix structure so as to create complementary arrays of hydrogen-bond donors and acceptors that, we hoped, would promote the formation of dimers of tertiary structures, i.e. genuine abiotic quaternary structures (Figures 2b,c, S3). An X7Y mutation was also introduced to avoid a possible steric clash in the dimers caused by the benzenic rings of X7. Similarly, Y was introduced in position 13 instead of X to avoid a steric clash (Figure S5a). Sequence **3b** is achiral, whereas an N-terminal (1*S*)-camphanyl group quantitatively biases the N-terminal helix of **2b** to *P* helicity.[31] Sequences **2a** and **3a**, the hydroxy group-protected precursors of **2b** and **3b**, were synthesized on solid phase using reported methods (see Supporting Information).[32,33] Introducing a glycine residue at the C-terminus and the use of 4-(hydroxymethyl)benzoyl-aminomethyl polystyrene (HMBA-AM) resin allowed to directly generate **2a** and **3a** as methyl esters upon sodium methoxide-mediated resin cleavage. The ^{1}H NMR spectra of protected sequences **2a** and **3a** in $CDCl_3$ showed two sets of signals corresponding to the *PM* and *PP* diastereomeric conformers of **2a** and the *PM*/*MP* and *PP*/*MM* conformers of **3a**, respectively, as expected for T2-containing precursors (Figure S6).[21] After side chain deprotection, the ^{1}H NMR

spectra of **2b** and **3b** in $CDCl_3$ showed only one set of sharp signals (Figure 1c), suggesting the formation of discrete species. Heating to 55 °C, changing the solvent to CD_2Cl_2, or diluting to 20 μM did not result in significant changes (Figures S7–S9). Eight (out of nine) O*H* resonances were identified as exchangeable protons showing no correlations to a ^{15}N atom in $^{1}H,^{15}N$ Heteronuclear Single Quantum Coherence (HSQC) NMR spectra (Figures 1c, S10, S11). Chemical shift values above 8.5 ppm indicated the involvement of these OH groups in hydrogen bonds. This pattern would be hard to fulfill intramolecularly, and it suggests the formation of a symmetrical aggregate too stable to dissociate at NMR concentrations in $CDCl_3$.[34]

A solid state structure[35] of achiral **3b** was obtained that differs from the initially-designed quaternary motif. Instead, it revealed a novel domain-swapped dimer (DSD) with an overall (non-crystallographic, Table S1) C_2-symmetry, in which the individual helix-turn-helix folds have been disrupted (Figures 2d, 3). Unlike **1**, the DSD consists of helical segments all having the same handedness. Furthermore, it contains exclusively intermolecular hydrogen bonds, entailing a massive structural reorganization with respect to the structure of **1** (Figures S12, S13). These hydrogen bonds can be divided into three areas (Table S2), two of which are characteristic of tilted helix-helix interactions (Figure 3c). As mentioned above, this mode of interaction had been previously identified.[20,22] Of note, the structure consists of so-called "counter-clockwise" tilts (Figure S4), whose existence had been hypothesized but had not yet been characterized. Only a "clockwise" tilt had been evidenced.[20,22] A third group of four hydrogen bonds was unexpected. It involves X4 and X9 hydroxy group donors, which are not present in **1** (blue arrows in Figures 2d and 3). The X4 hydroxy protons hydrogen bond to carbonyl groups of T2 units (Figure S2), which themselves undergo a conformation change. Indeed, instead of the flat, conjugated diacylhydrazine conformation that prevails in helix-turn-helix motifs, the diacylhydrazine N–N bonds of T2 units are twisted by around 90° in the DSD.[36] It is this twist at the center of each molecule that orients the helices to enable the formation of the tilted interfaces. Altogether, it appears that the DSD is favored by: (*i*) the more stable tilted helix-helix interface as opposed to the frustrated helix-helix interface with parallel helix axes; (*ii*) intermolecular hydrogen bonds involving donors not present in **1**; (*iii*) a twist of the diacylhydrazine group; (*iv*) the X7Y and the Q13Y mutations without which the DSD would cause steric clashes (Figure S5b,c). However, the DSD formed despite the fact that two Y13 OH groups are not involved in hydrogen bonds (red arrows in Figures 2d and 3, Figure S14).[37]

The ^{1}H NMR spectra of **2b** and **3b** are consistent with the solid state structure of $(\mathbf{3b})_2$. The number of signals aligns with the symmetry of the DSD.[34] The ^{15}N chemical shifts for the diacylhydrazine group are found at 114 and 116 ppm (Figure S10), considerably shifted from their values for compound **1** (at 126 and 128 ppm),[21] which is in agreement with a change of conformation. The count of O*H* signals in solution (Figure 1c) supports that one O*H* is not hydrogen-bonded (that of Y13 in the DSD). Adding 4 vol %

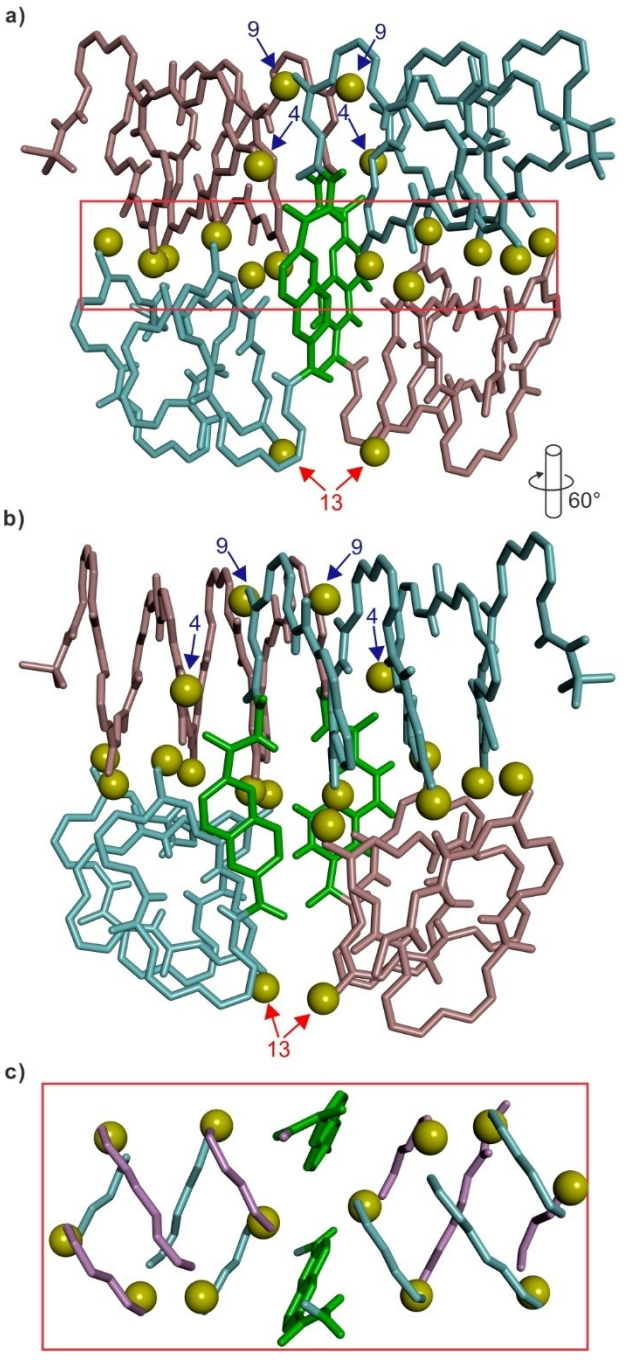

Figure 3. a, b) Simplified views of the solid state structure of $(\mathbf{3b})_2$ as a domain-swapped dimer. Only the all *P* structure is shown. The crystal lattice is centrosymmetrical and also contains the all *M* enantiomer. Individual molecules are shown in light blue and pink tube representation. Hydroxy protons are shown as yellow balls. T2 linkers are shown in green. For clarity, only the outer rim of the helices is shown. The side chains of Q and T2 have been omitted. Blue arrows point to unexpected hydrogen bonds. Red arrows point to hydroxy groups not involved in hydrogen bonds. c) Top view of the intermolecular interface located in the red box in a) showing the two hexagonal arrangement of hydrogen bond donors associated with the tilted helix-helix interaction. Color coding is as in a) and b).

of DMSO-d_6 to a $CDCl_3$ solution of **2b** caused little changes to the ^{1}H NMR spectrum except for the appearance of an additional O*H* signal above 8.5 ppm (Figure S15), consistent with this proton not being hydrogen-bonded within **2b** but shifting downfield upon hydrogen bonding to DMSO. Furthermore, upon varying the concentration of **2b** in DMSO-d_6/$CDCl_3$ (4:96, vol/vol), two sets of signals are observed in varying proportions (Figure 4b). These changes, as well as Diffusion Ordered SpectroscopY (DOSY, Figure 4c), demonstrate that the species that prevails in $CDCl_3$ is an aggregate. Assuming a monomer/dimer equilibrium, we calculated $K_{dim} = 6.3 \cdot 10^{-5}$ L mol^{-1} in this solvent. The absence of dissociation at NMR concentrations in pure $CDCl_3$ (Figure S7), i.e. a much higher K_{dim}, is consistent with the stability of other hydrogen-bonded dimers we have described.[20,30] Increasing the fraction of DMSO-d_6 above 4 vol% further favored the formation of the monomer (Figures 4b, S16). Above 10 vol%, another set of signals appeared that eventually became major at 20 vol%. This amount of DMSO-d_6 has previously been shown to disrupt the hydrogen bond interface of **1**.[21] A model that would explain the results above is shown in Figure 4a. A small amount of DMSO-d_6 causes the DSD dissociation into a folded monomer having a *P* and an *M* helix. Adding further DMSO-d_6 disrupts the intramolecular helix-helix interface and produces a monomer with two *P* helices.

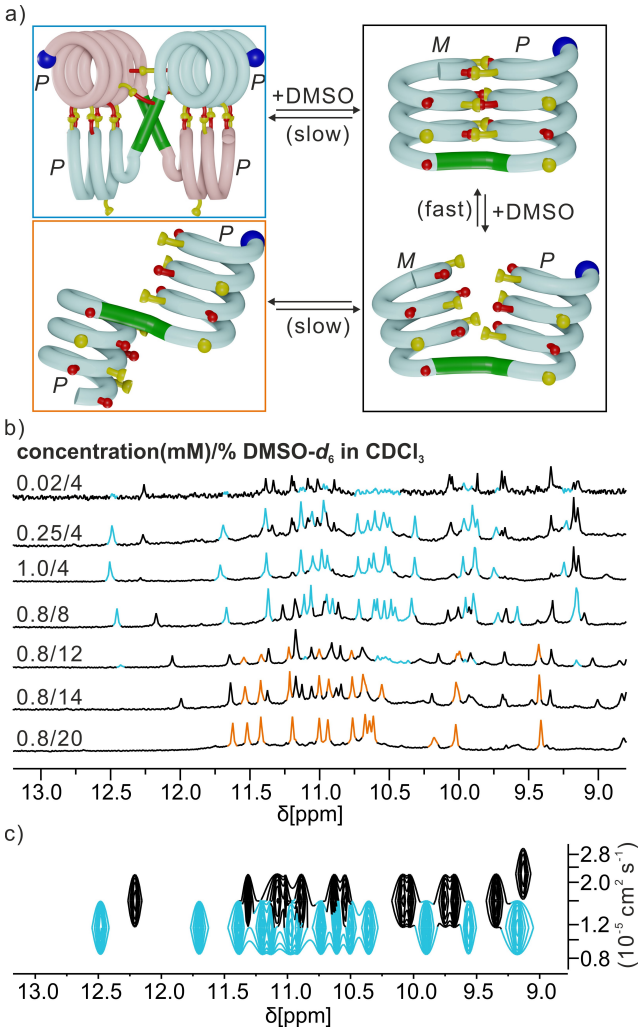

Figure 4. a) Schematic representation of changes induced upon adding DMSO to a solution of DSD. The slow or fast rates are with respect to the NMR time scale. Stoichiometry (a dimer gives two monomers) has been omitted for clarity. b) Excerpts of the ^{1}H NMR spectra (500 MHz, 25 °C) of **2b** in DMSO-d_6/$CDCl_3$ at different concentrations and different vol% of DMSO-d_6. c) 500 MHz DOSY ^{1}H NMR spectrum of **2b** at 25 °C, 1 mM in DMSO-d_6/$CDCl_3$ (10:90 v/v). In b) and c) peaks are colored according to the species they belong to, as coded in the boxes shown in a).

The effect of DMSO on the CD spectra of **2b** corroborated the NMR data. In pure $CHCl_3$, the CD spectrum of **2b** showed an intense positive band at 400 nm belonging to the quinoline chromophores and indicating the prevalence of *P* helicity (Figure 5a) as expected in the DSD.[31] Adding DMSO caused a drop in CD intensity of about 60%, consistent with the appearance of the *PM* folded monomer. In the *PM* conformation, the CD contribution of the *P* helix and the *M* helix almost entirely cancel each other for the helices have similar numbers of quinoline rings. Further addition of DMSO resulted in the CD band intensity growing again as the *PM* conformer was disrupted to produce some *PP* monomer (Figures 4a, 5a,b). Finally, **4b** and **5b** were produced as analogues of **2b** and **3b**, respectively. These two sequences lack one hydroxy group as the monomer in position 13 is P instead of Y (Figure 1a, b). Nevertheless, **4b** and **5b** behaved like **2b** and **3b** in all respects in solution (Figures 1c, S17–S21). Altogether, these results strongly support that the DSD observed in the solid state structure of $(\mathbf{3b})_2$ corresponds to the species in $CDCl_3$ solutions of **2b**, **3b**, **4b**, and **5b**.

DSD formation reflects the ability of a folded structure to respond to changes. As was recently illustrated, the change may be the presence of a guest molecule.[4] Here, it is

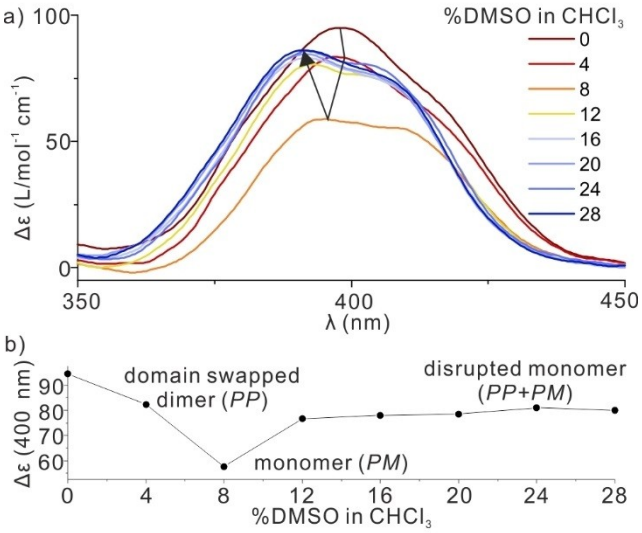

Figure 5. a) CD spectra of **2b**, 0.1 mM in $CHCl_3$ with different proportions of DMSO. b) The Δε values at 400 nm extracted from a) as a function of the vol% of DMSO in $CHCl_3$.

the consequence of a few mutations. Current efforts in our laboratories intend to exploit both the responsiveness and the geometry of DSD's. Meanwhile, progress to genuine quaternary structures has been made and will be reported in due course.

Supporting Information

The authors have cited additional references within the Supporting Information.[38–45]

Acknowledgements

We acknowledge financial support from the China Scholarship Council (CSC, predoctoral fellowship to S.W.). This work has benefited from the facilities and expertise of the Biophysical and Structural Chemistry platform (BPCS) at IECB, CNRS UMS3033, Inserm US001, and Bordeaux University. We thank B. Kauffmann for assistance with X-ray data collection, F. Menke for advice with synthesis, L. Allmendinger for some NMR measurements, and D. Gill for providing some precursors. Open Access funding enabled and organized by Projekt DEAL.

Conflict of Interest

The authors declare no conflict of interest.

Keywords: abiotic foldamer · domain swapping · hydrogen bonding · structure elucidation · tertiary structure

[1] W. Wang, C. Zhang, S. Qi, X. Deng, B. Yang, J. Liu, Z. Dong, *J. Org. Chem.* **2018**, *83*, 1898–1902.
[2] Y. Hua, Y. Liu, C. H. Chen, A. H. Flood, *J. Am. Chem. Soc.* **2013**, *135*, 14401–14412.
[3] N. Chandramouli, Y. Ferrand, G. Lautrette, B. Kauffmann, C. D. Mackereth, M. Laguerre, D. Dubreuil, I. Huc, *Nat. Chem.* **2015**, *7*, 334–341.
[4] G. Song, S. Lee, K.-S. Jeong, *Nat. Commun.* **2024**, *15*, 1501.
[5] J. Shen, Z. Li, H. Oh, H. Behera, H. Joshi, M. Kumar, A. Aksimentiev, H. Zeng, *Angew. Chem. Int. Ed.* **2023**, *62*, e202305623; *Angew. Chem.* **2023**, *135*, e202305623.
[6] J. Shen, R. Ye, Z. Liu, H. Zeng, *Angew. Chem. Int. Ed.* **2022**, *61*, e202200259; *Angew. Chem.* **2022**, *134*, e202200259.
[7] L. Zhang, C. Zhang, X. Dong, Z. Dong, *Angew. Chem. Int. Ed.* **2023**, *62*, e202214194; *Angew. Chem.* **2023**, *135*, e202214194.
[8] Y. Shen, F. Fei, Y. Zhong, C. Fan, J. Sun, J. Hu, B. Gong, D. M. Czajkowsky, Z. Shao, *ACS Cent. Sci.* **2021**, *7*, 2092–2098.
[9] S. Qi, C. Zhang, H. Yu, J. Zhang, T. Yan, Z. Lin, B. Yang, Z. Dong, *J. Am. Chem. Soc.* **2021**, *143*, 3284–3288.
[10] I. Huc, *Eur. J. Org. Chem.* **2004**, *2004*, 7–7.
[11] D.-W. Zhang, X. Zhao, J.-L. Hou, Z.-T. Li, *Chem. Rev.* **2012**, *112*, 5271–5316.
[12] Y. Hamuro, S. J. Geib, A. D. Hamilton, *Angew. Chem. Int. Ed.* **1994**, *33*, 446–448; *Angw. Chem.* **1994**, *106.* 465–467.
[13] J. Zhu, R. D. Parra, H. Zeng, E. Skrzypczak-Jankun, X. C. Zeng, B. Gong, *J. Am. Chem. Soc.* **2000**, *122*, 4219–4220.
[14] B. Gong, H. Zeng, J. Zhu, L. Yua, Y. Han, S. Cheng, M. Furukawa, R. D. Parra, A. Y. Kovalevsky, J. L. Mills, *Proc. Natl. Acad. Sci. USA* **2002**, *99*, 11583–11588.
[15] Z.-Q. Wu, X.-K. Jiang, S.-Z. Zhu, Z.-T. Li, *Org. Lett.* **2004**, *6*, 229–232.
[16] J. T. Ernst, J. Becerril, H. S. Park, H. Yin, A. D. Hamilton, *Angew. Chem. Int. Ed.* **2003**, *42*, 535–539; *Angew. Chem.* **2003**, *115*, 553–557.
[17] V. Maurizot, C. Dolain, Y. Leydet, J.-M. Léger, P. Guionneau, I. Huc, *J. Am. Chem. Soc.* **2004**, *126*, 10049–10052.
[18] N. Delsuc, S. Massip, J.-M. Léger, B. Kauffmann, I. Huc, *J. Am. Chem. Soc.* **2011**, *133*, 3165–3172.
[19] C. Dolain, J.-M. Léger, N. Delsuc, H. Gornitzka, I. Huc, *Proc. Natl. Acad. Sci. USA* **2005**, *102*, 16146–16151.
[20] S. De, B. Chi, T. Granier, T. Qi, V. Maurizot, I. Huc, *Nat. Chem.* **2018**, *10*, 51–57.
[21] D. Mazzier, S. De, B. Wicher, V. Maurizot, I. Huc, *Angew. Chem. Int. Ed.* **2020**, *59*, 1606–1610; *Angew. Chem.* **2020**, *132*, 1623–1627.
[22] F. S. Menke, B. Wicher, L. Allmendinger, V. Maurizot, I. Huc, *Chem. Sci.* **2023**, *14*, 3742–3751.
[23] D. Mazzier, S. De, B. Wicher, V. Maurizot, I. Huc, *Chem. Sci.* **2019**, *10*, 6984–6991.
[24] F. S. Menke, D. Mazzier, B. Wicher, L. Allmendinger, B. Kauffmann, V. Maurizot, I. Huc, *Org. Biomol. Chem.* **2023**, *21*, 1275–1283.
[25] Y. Huang, H. Cao, Z. Liu, *Proteins* **2012**, *80*, 1610–1619.
[26] N. Nandwani, P. Surana, H. Negi, N. M. Mascarenhas, J. B. Udgaonkar, R. Das, S. Gosavi, *Nat. Commun.* **2019**, *10*, 452.
[27] D. Sanchez-Garcia, B. Kauffmann, T. Kawanami, H. Ihara, M. Takafuji, M.-H. Delville, I. Huc, *J. Am. Chem. Soc.* **2009**, *131*, 8642–8648.
[28] C. Dolain, A. Grélard, M. Laguerre, H. Jiang, V. Maurizot, I. Huc, *Chem. Eur. J.* **2005**, *11*, 6135–6144.
[29] H. Jiang, J.-M. Léger, I. Huc, *J. Am. Chem. Soc.* **2003**, *125*, 3448–3449.
[30] F. S. Menke, B. Wicher, V. Maurizot, I. Huc, *Angew. Chem. Int. Ed.* **2023**, *62*, e202217325; *Angew. Chem.* **2023**, *135*, e202217325.
[31] A. M. Kendhale, L. Poniman, Z. Dong, K. Laxmi-Reddy, B. Kauffmann, Y. Ferrand, I. Huc, *J. Org. Chem.* **2011**, *76*, 195–200.
[32] B. Baptiste, C. Douat-Casassus, K. Laxmi-Reddy, F. Godde, I. Huc, *J. Org. Chem.* **2010**, *75*, 7175–7185.
[33] V. Corvaglia, F. Sanchez, F. S. Menke, C. Douat, I. Huc, *Chem. Eur. J.* **2023**, *29*, e202300898.
[34] Earlier systems showed that exchange between different aggregates or between aggregate and monomer is slow on the NMR times scale. If an aggregate was not symmetrical, different resonances would be seen for the different subunits. See Ref. [20].
[35] Deposition Number 2337052 (for **3b**) contain(s) the supplementary crystallographic data for this paper. These data are provided free of charge by the joint Cambridge Crystallographic Data Centre and Fachinformationszentrum Karlsruhe Access Structures service.
[36] Such a twisted diacylhydrazine has been observed before. See Ref. [3].
[37] The preference for the tilted hydrogen-bonded helix-helix interface has already been observed to be strong enough to compensate for some orphan OH groups. See Ref. [20].
[38] Rigaku-Oxford-Diffraction, *CrysAlisPro Software System, Version 171.42.79a*, **2022**, Rigaku Corporation: Yarton, England.
[39] G. M. Sheldrick, *Acta Crystallogr.* **2015**, *A71*, 3–8.
[40] G. M. Sheldrick, *Acta Crystallogr.* **2015**, *C71*, 3–8.
[41] O. V. Dolomanov, L. J. Bourhis, R. J. Gildea, J. A. K. Howard, H. Puschmann, *J. Appl. Crystallogr.* **2009**, *42*, 339–341.

[42] V. Corvaglia, F. Sanchez, F. S. Menke, C. Douat, I. Huc, *Chem. Eur. J.* **2023**, *29*, e202300898.
[43] M. Vallade, P. Sai Reddy, L. Fischer, I. Huc, *Eur. J. Org. Chem.* **2018**, *2018*, 5489–5498.
[44] O. Al Musaimi, A. Basso, B. G. de la Torre, F. Albericio, *ACS Comb. Sci.* **2019**, *21*, 717–721.
[45] J. Hansen, F. Diness, M. Meldal, *Org. Biomol. Chem.* **2016**, *14*, 3238–3245.

Manuscript received: March 14, 2024
Accepted manuscript online: April 25, 2024
Version of record online: June 4, 2024